



Study of the cosmic ray primary spectrum at $10^{15} < E_0 < 10^{16}$ eV with the EAS-TOP array

M. Aglietta^{1,2}, B. Alessandro², P. Antonioli³, F. Arneodo⁴, L. Bergamasco^{2,5}, M. Bertaina^{2,5}, C. Castagnoli^{1,2}, A. Castellina^{1,2}, A. Chiavassa^{2,5*}, G. Cini Castagnoli^{2,5}, B. D'Ettorre Piazzoli⁶, G. Di Sciascio⁶, W. Fulgione^{1,2}, P. Galeotti^{2,5}, P.L. Ghia^{1,2}, M. Iacovacci⁶, A. Lima de Godoi⁷, G. Mannocchi^{1,2}, C. Morello^{1,2}, G. Navarra^{2,5}, O. Saavedra^{2,5}, G.C. Trincheri^{1,2}, S. Valchierotti^{2,5}, P. Vallania^{1,2}, S. Vernetto^{1,2} and C. Vigorito^{1,2}

¹*Istituto di Cosmo-Geofisica del CNR, Torino, Italy*

²*Istituto Nazionale di Fisica Nucleare, Torino, Italy*

³*Istituto Nazionale di Fisica Nucleare, Bologna, Italy*

⁴*INFN, Laboratorio Nazionale del Gran Sasso, L' Aquila, Italy*

⁵*Dipartimento di Fisica Generale dell' Università, Torino, Italy*

⁶*Dipartimento di Scienze Fisiche dell' Università and INFN, Napoli, Italy*

⁷*Universidade de São Paulo, São Paulo, Brasil*

The break observed in the electron shower size power law spectrum of Extensive Air Showers (EAS) at corresponding primary energy $E_0 \sim (3 - 5)10^{15}$ eV ("knee") is studied in different EAS components (electromagnetic and muonic) and at different atmospheric depths. A consistent description is obtained. The interpretation of data in terms of primary composition, and following the most accepted high energy interaction models, leads to an increasing average primary mass in this energy range. The study of such behaviour is expected to provide a crucial information for the understanding of the physical parameters that characterize the break for the different primaries.

1. INTRODUCTION

The cosmic ray primary spectrum is well described by a power law over a very wide range of primary energies. Measurements are performed with different techniques: direct (experiments operating on satellites or balloons, at energies $E_0 < 10^{13}$ eV) and indirect (ground based arrays detecting different components of Extensive Air Showers, EAS, at $E_0 > 10^{14} - 10^{15}$ eV). The most interesting feature is represented by the change of slope (better known as the knee) measured [1] by means of the detection of the electromagnetic component of EAS, at primary energies $E_k = (3 - 5) \times 10^{15}$ eV. Such energy exceeds the maximum energy reached by colliders (Tevatron, limited to $p-\bar{p}$ collisions and to the central rapidity region).

The analysis of Extensive Air Shower experiments, aimed at measuring the primary spectrum

and composition around (and above) the knee, depend therefore on properties of hadronic interactions not directly measured but extrapolated through theoretical or phenomenological models. Experiments have therefore to test the main features of such models through measurements as far as possible independent from the primary composition. In presence of a spectral feature as the knee an internal consistency of the data, obtained on different EAS components, has to be established in order to exclude its origin from "new" hadronic interaction effects.

Furthermore the evolution of the chemical composition, which is considered a main tool to test different astrophysical hypothesis [2] proposed to explain the knee, can be studied.

The former goal has been faced through studies of the spectra of different secondary components of EAS at different atmospheric depths (i.e. spectra measured, by a single array, at different zenith angles). In fact, if the change in slope is a char-

*e-mail achiavas@to.infn.it

acteristic of an energy (E_k) and a mass (A_k), its observation at different atmospheric depths has to be consistent for the different EAS components.

In this paper we present the results obtained with the EAS-TOP experiment on the N_e and N_μ spectra at different atmospheric depths, their comparison and a study of the primary chemical composition through the N_e - N_μ relation.

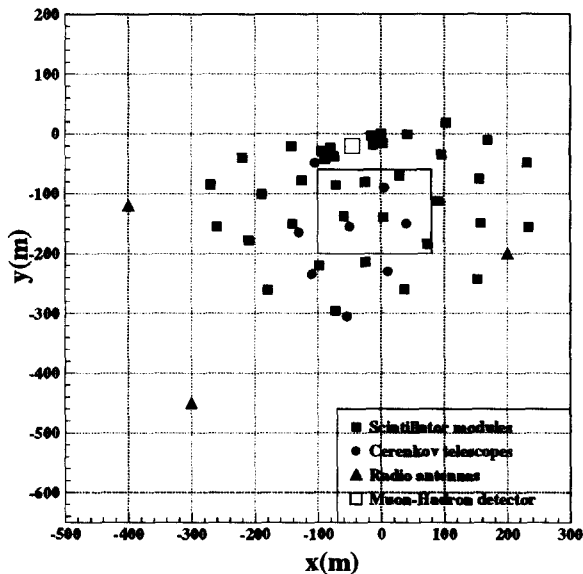


Figure 1. The EAS-TOP array. The inner box shows the area used to select events for the measurement of N_e spectra.

2. THE EXPERIMENT

The EAS-TOP array is located at Campo Imperatore, 2005 m a.s.l. (above the underground Gran Sasso laboratories), at 810 g cm^{-2} atmospheric depth. The electromagnetic detector [3] is made of 35 scintillator modules, 10 m^2 each, separated by 20 m in the central region and 80 m at the edges of the array (see fig. 1).

Event selection, for the analysis discussed in this work, requires at least 6 (or 7) modules fired (with threshold, for each module, set at $1/3$ of the signal due to a minimum ionizing particle) and the highest particle density recorded by an inner module, i.e. a module not located at the edges of the array.

The core location, the slope (s) of the lateral distribution function (ldf in the following) and the shower size are obtained by means of a minimum χ^2 fit to the theoretical NKG ldf [4]:

$$\rho_e(r) = N_e \frac{C(s)}{r_0^2} \left(\frac{r}{r_0}\right)^{s-2} \left(1 + \frac{r}{r_0}\right)^{s-4.5} \text{ m}^{-2} \quad (1)$$

with $r_0 = 100 \text{ m}$.

The accuracy in the measurement of the shower size has been obtained by analyzing simulated data, including experimental dispersions. The dependence of $\Delta N_e/N_e$ on N_e is shown in fig. 2, being $\Delta N_e/N_e \sim 10\%$ in the region of interest for the present analysis.

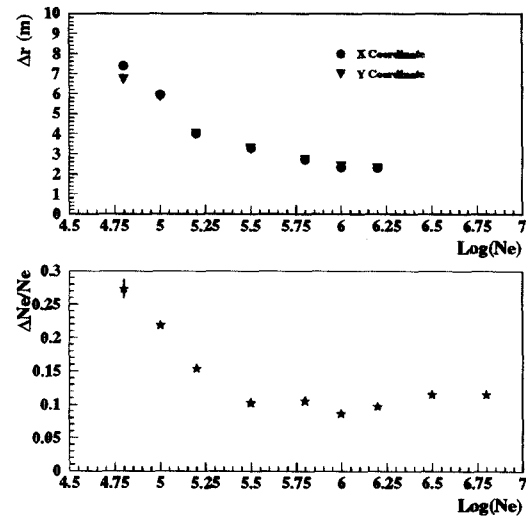


Figure 2. Accuracy in the determination of the core location (Δr) and of the shower size ($\Delta N_e/N_e$) vs N_e . Events have been simulated with zenith angle θ between 0° and 40° ; no dependence of the reconstruction accuracy on θ is observed in such range.

The muon detector [5] covers a surface of 144 m^2 and consists of 9 identical planes. Each plane is made of two layers of streamer tubes (for muon tracking) and one layer of tubes operating in "quasi proportional" regime (for hadron calorimetry). Planes are separated by 13 cm thick iron absorbers. On each plane the x coordinate of muon track is obtained from the signals of the anode wires (368 in a layer), the y one from the induced signals on strips orthogonal to the wires.

The tube sections are $3 \times 3 \text{ cm}^{-2}$ and the strip widths are 3 cm. A muon track is defined from the alignment of at least 6 hits (wires on) in different layers of tubes. The muon energy threshold for vertical events is $E_{\mu}^{thr} = 1 \text{ GeV}$. The muon density $\rho_{\mu}(r, E_{\mu} > 1 \text{ GeV})$, with r obtained from the e.m. detector data, is thus measured.

3. RESULTS

3.1. Ne spectra

The analysis has been performed using all events with zenith angle $\theta < 40^{\circ}$ and core located inside the internal area shown in fig. 1 (defined requiring a detection efficiency $> 95\%$ for $\text{Log}(Ne) > 5.2$). The data set is equivalent to ~ 257 days of live time.

Fig. 3 shows the differential size spectra measured in six different intervals of zenith angle (width $\Delta \sec \theta = 0.05$, i.e. $\Delta x \sim 40 \text{ g cm}^{-2}$ at the depth of EAS-TOP); data being corrected for the effects of detector dispersions.

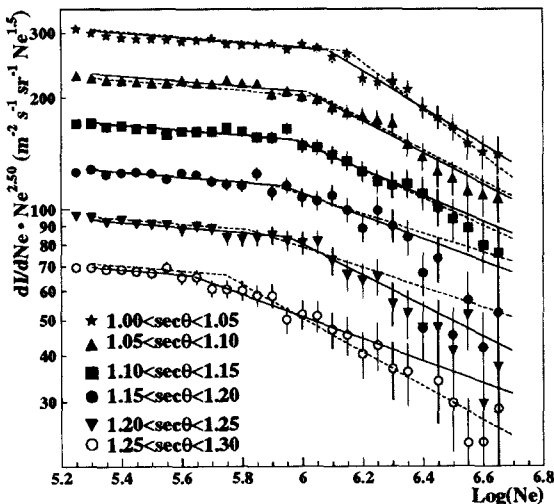


Figure 3. Differential shower size spectra measured at different atmospheric depths. Spectra are multiplied by $Ne^{2.5}$ to emphasize the change of slope at the knee. Solid lines: independent fits, dashed lines: fit requiring equal integral fluxes above the knee.

The parameters of the different spectra are obtained through independent fits according to the

following expression:

$$I(Ne, \theta) = I_k(\theta) \left(\frac{Ne}{Ne_k(\theta)} \right)^{-\gamma_{1,2}(\theta)} \quad (2)$$

where γ_1 and γ_2 are the spectral indexes below and above the knee. I_k is the differential flux and Ne_k the shower size at the knee. Results are reported in tab. 1 and shown in fig. 3 by solid lines.

The main features obtained from the fits, as a function of zenith angle (i.e. of the atmospheric depth) are:

- the slope below the knee is constant (inside experimental errors) and with mean value $\bar{\gamma}_1 = 2.56 \pm 0.02$ [6];
- the integral intensity above the knee ($I(> Ne_k)$) is constant inside the experimental uncertainties;
- the size at the knee (Ne_k) decreases with increasing atmospheric depth.

In general an expression as (2) with a sharp intersection of two power laws at the break is a good representation of the data showing that the change in slope occurs in a limited range of Ne (i.e. in $\Delta Ne/Ne \leq 25\%$).

The attenuation length of Ne_k has been obtained through a common fit of all spectra with the conditions: $I(> Ne_k)$ constant, $Ne_k \propto Ne_k(0^\circ) e^{-(x-x_0)}/\Lambda_k$ and $\gamma_1 = \bar{\gamma}_1$. In this frame the free parameters are: $Ne_k(0^\circ)$, $I(> Ne_k)$, Λ_k and the slopes γ_2 above the knee. The obtained values are: $I(> Ne_k) = (8.1 \pm 0.7) \times 10^{-8} \text{ m}^{-2} \text{ s}^{-1} \text{ sr}^{-1}$, $\text{Log} Ne_k(0^\circ) = 6.15 \pm 0.02$, and $\Lambda_k = 222 \pm 3 \text{ g cm}^{-2}$, a value which is in excellent agreement with the attenuation length obtained for EAS particles with the constant intensity cut technique ($\Lambda_{EAS} = 219 \pm 3 \text{ g cm}^{-2}$). The results of this fitting procedure are shown in fig. 3 by dashed lines.

3.2. $N\mu$ spectra

Muon number spectra are measured in the first four intervals of zenith angles. In order to limitate effects due to inaccuracies of the used ldf events are selected inside a narrow range of distances from the μ detector: $140 < r < 170 \text{ m}$ ($A_f \sim 6 \times 10^3 \text{ m}^2$). Large statistical fluctuations and saturation problems are avoided using event

Table 1

Results obtained from the fits to the Ne spectra measured in different bins of zenith angle.

$\Delta \text{sec } \theta$	γ_1	γ_2	$I(> Ne_k) \times 10^7$ $\text{m}^{-2} \text{s}^{-1} \text{sr}^{-1}$	$\text{Log}(Ne_k)$
1.00 – 1.05	2.56 ± 0.02	2.99 ± 0.09	0.99 ± 0.2	6.09 ± 0.05
1.05 – 1.10	2.55 ± 0.02	2.93 ± 0.11	1.01 ± 0.3	6.02 ± 0.07
1.10 – 1.15	2.55 ± 0.03	2.85 ± 0.12	0.93 ± 0.4	5.97 ± 0.08
1.15 – 1.20	2.56 ± 0.03	2.81 ± 0.16	0.80 ± 0.4	5.93 ± 0.14
1.20 – 1.25	2.59 ± 0.03	2.91 ± 0.26	0.52 ± 0.3	5.95 ± 0.11
1.25 – 1.30	2.55 ± 0.07	2.80 ± 0.11	1.30 ± 0.6	5.63 ± 0.12

with tracks numbers between 8 and 35. This allows to measure, in the chosen r interval, muon densities $0.05 < \rho_\mu < 0.29 \text{ m}^{-2}$, converted for easier interpretation to the muon size ($N\mu$) in the range $4.50 < \text{Log}(N\mu) < 5.15$.² The obtained spectra (corresponding to a data set of 278 days of data taking), are shown in fig. 4; the change of slope is visible in all of them in spite of the large statistical fluctuations.

The spectral slopes below and above the knee and the muon density at the knee are obtained through a minimum χ^2 procedure comparing the experimental data to a trial spectrum taking into account the poissonian fluctuations of the number of detected muons. The integral flux above the knee ($I(> N\mu_k)$) is obtained from the total number of events with $N\mu > N\mu_k$. Results are shown in tab. 2; the value of the total muon number ($N\mu_k$), corresponding to the change of slope, calculated from the muon density at the knee using the muon ldf (3) is also given.

3.3. Comparison of the Ne and $N\mu$ data

From the comparison of the parameters of the Ne and $N\mu$ spectra we obtain:

- a) the integral fluxes above the knee $I(> Ne_k)$ and $I(> N\mu_k)$ are consistent, inside the experimental uncertainties, at all atmospheric depths;
- b) the Ne_k and $N\mu_k$ error boxes fall well inside the experimental $Ne - N\mu$ scatter plot (with statistical and systematic uncertainties still not allowing conclusions on the primary mass at the knee), see fig. 5;
- c) the slopes γ_1 and γ_2 , below and above the knee are connected by a relation $N\mu \propto Ne^\alpha$ with $\alpha \sim 0.7 - 0.8$ as predicted by most models (see fig. 6).

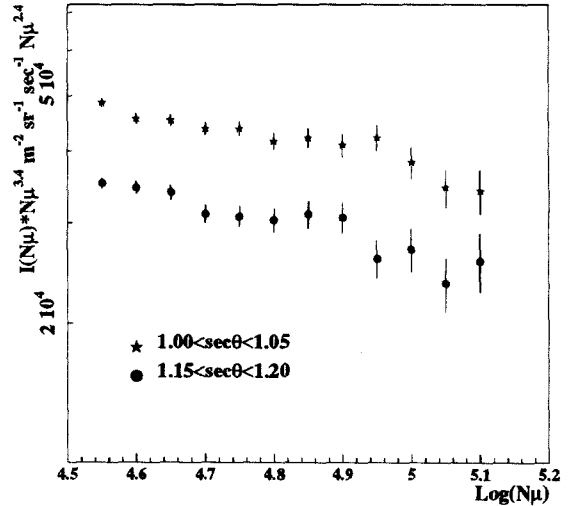


Figure 4. $N\mu$ spectra measured in different bins of zenith angles, i.e. at different atmospheric depths.

These data are generally consistent and show that, at the present stage, no "new" hadronic physics effect are required to describe the knee.

3.4. The primary composition

Figure 7 shows the behaviour of the mean value $\overline{N\mu}$ observed, in vertical direction, in narrow bins of Ne ($\Delta \text{Log}(Ne) = 0.05$). The experimental results (160 days of data taking) are compared with

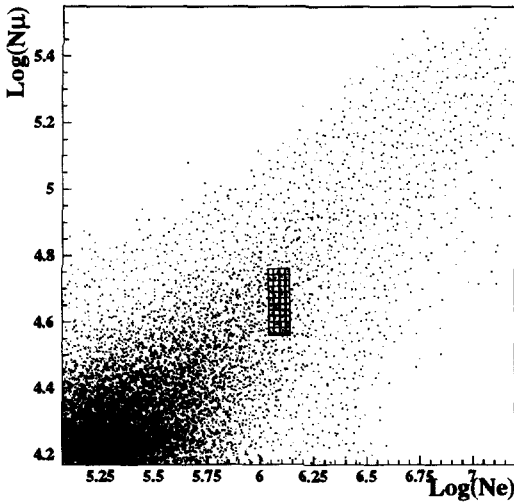
²The muon size ($N\mu$) is calculated using the average muon ldf , ($r_0 = 300 \text{ m}$):

$$N\mu = \rho_\mu(r) \frac{r_0^{1.25} r^{0.75}}{0.269} \left(1 + \frac{r}{r_0} \right)^{2.5} \quad (3)$$

Table 2

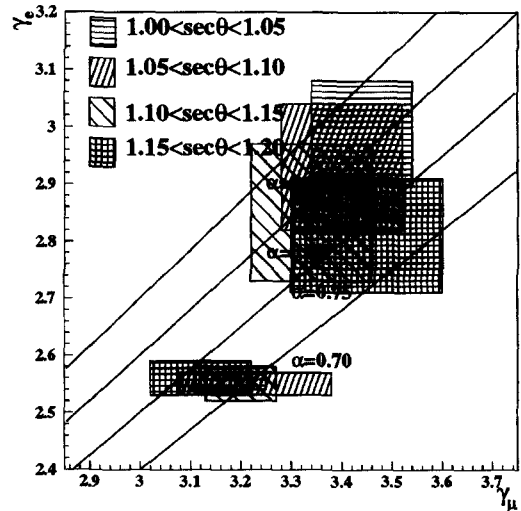
Results obtained on the parameters of the $N\mu$ spectra measured at different zenith angles.

$\Delta \text{sec } \theta$	γ_1	γ_2	$\rho_\mu(r = 150\text{m})$ m^{-2}	$\text{Log}(N\mu_k)$	$I(> N\mu_k) \times 10^7$ $\text{m}^{-2} \text{s}^{-1} \text{sr}^{-1}$
1.00 – 1.05	3.18 ± 0.07	3.44 ± 0.10	0.08 ± 0.02	4.66 ± 0.10	1.32 ± 0.3
1.05 – 1.10	3.23 ± 0.15	3.40 ± 0.12	0.07 ± 0.02	4.62 ± 0.10	1.03 ± 0.3
1.10 – 1.15	3.20 ± 0.07	3.34 ± 0.12	0.08 ± 0.02	4.65 ± 0.12	1.09 ± 0.3
1.15 – 1.20	3.12 ± 0.10	3.45 ± 0.15	0.07 ± 0.02	4.60 ± 0.10	1.28 ± 0.3

Figure 5. Scatter plot of experimental $Ne - N\mu$ data for vertical direction. The knee location error box is shown

the results of a complete shower simulation including detectors' responses. In the simulation the 1 TeV composition is used with equal slopes ($\gamma = 2.75$) for all components (thus reproducing a sample with a value of \bar{A} constant with energy). It appears that the experimental measurements of $\bar{N}\mu$ shift systematically towards higher values with respect to the simulated ones for increasing Ne , indicating a growth of \bar{A} with energy. The difference between the measured and simulated values of $N\mu$ ($\Delta\bar{N}\mu$) is, for $\Delta\text{Log}(Ne) = 1$: $\Delta\bar{N}\mu/\bar{N}\mu \approx 0.17$.

This result depends on the hadronic interaction model; the used one (HDPM) provides very good agreement with other independent EASTOP measurements [7] and moreover other models (as e.g. QGSJET) provide similar result re-

Figure 6. Relation between the slopes of the Ne and $N\mu$ spectra measured below and above the knee.

quiring an even larger increase of $\Delta\bar{A}/\bar{A}$.

3.5. The energy spectrum

The all particle energy spectrum is obtained (see fig. 8), from all events with $\theta < 40^\circ$, converting every shower size to 810 g cm^{-2} using Λ_{EAS} . The conversion from primary energy (E_0 , in TeV) and mass (A) to shower size has been obtained by means of complete simulations of cascades in atmosphere using the CORSIKA-HDPM code [8]:

$$Ne(E_0, A) = \alpha(A) E_0^{\beta(A)} \quad (4)$$

where $\alpha(A) = 197.5A^{-0.521}$, and $\beta(A) = 1.107A^{0.035}$. The effective value of the primary mass is calculated from the extrapolation of the single nuclear spectra measured at lower energies by experiments operating at the top of the atmo-

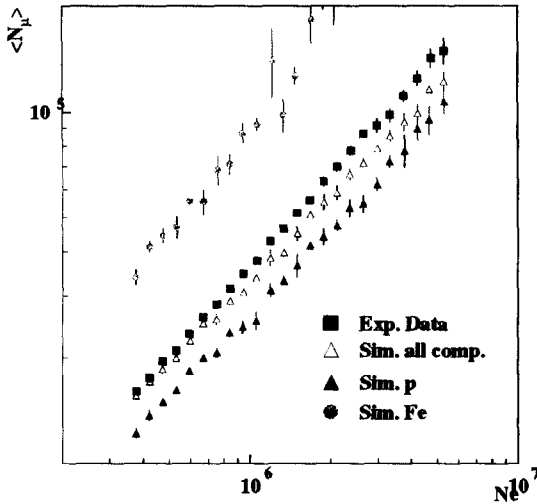


Figure 7. $N\mu$ vs N_e relation for experimental data and a composition with the same slope ($\gamma = 2.75$) for all components. Pure proton and pure iron simulated data are also plotted for comparison.

sphere, and using (above the knee) a rigidity dependent cutoff: $\Delta\gamma = 0.4$ for $E_k(A) = Z \cdot 2 \cdot 10^{15}$ eV. The used values range from $A_{eff} = 10^{5.2}$, $A_{eff} = 8.9$ for $N_e = 10^{6.0}$ to $A_{eff} = 10.9$ for $N_e = 10^{6.5}$.

The knee energy (E_{0k}), obtained from expression (4) and $N_{e_k} = 10^{6.09}$, is $E_{0k} = 2.74$ PeV for $A = 1$, $E_{0k} = 3.4$ PeV ($A = 4$), $E_{0k} = 4.1$ PeV ($A = 14$), $E_{0k} = 4.9$ PeV ($A = 56$).

4. CONCLUSIONS

The EAS-TOP measurements of the e.m. and muon EAS components at different atmospheric depths in the knee region provide a consistent experimental scenario: the values at the break, their attenuation in atmosphere, the spectral indexes and the intensities above the knee of the electron and muon size spectra show good compatibility.

The slope of the primary spectrum changes from $\gamma_1 = 2.76 \pm 0.03$ to $\gamma_2 = 3.19 \pm 0.06$ around the knee. The energy corresponding to the knee is $E_k = (2.7 \div 4.9) \times 10^{15}$ eV.

The N_e - $N\mu$ relation indicates an increasing average primary mass in this energy range. The amount of such variation is model dependent, but its occurrence is confirmed by different interaction

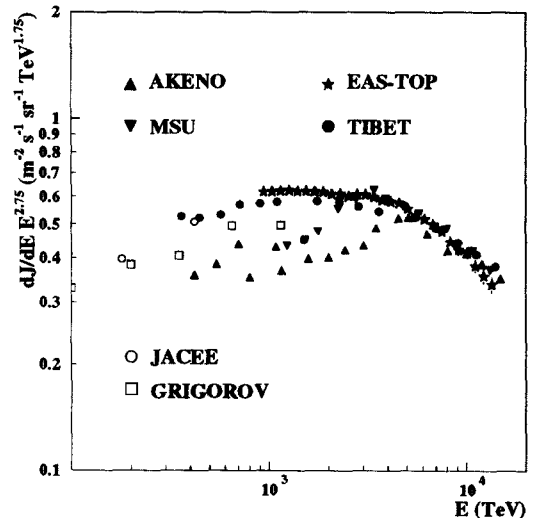


Figure 8. The all particle energy spectrum obtained from the EAS-TOP shower size data, compared with the results of other experiments operating outside the atmosphere or at ground level.

models.

REFERENCES

1. G. Kulikov & G.B. Khristiansen, JEPT, **35**, 635 (1958)
2. B. Peters, Proc. 23rd ICRC, Moscow, **3**, 157 (1959); G.T. Zatsepin et al., Izv. Ak. Nauk USSR, SP, **26**, 685 (1962); A.M. Hillas, Proc. of 16th ICRC (Kyoto), **8**, 7 (1970); P.L. Biermann, Proc. 23rd ICRC, Calgary, *Invited, Rapporteur and Highlight papers*, 45 (1994); A.D. Erlykin & A.W. Wolfendale, J. Phys. G., **23**, 979 (1997); *Astrop. Phys.*, **7**, 1 (1997)
3. M. Aglietta et al., N.I.M. A, **336** (1993) 310
4. K. Kamata et al., *Suppl. Progr. Theor. Phys.*, **6** (1958) 93
5. Aglietta M. et al., N.I.M. A, **420** (1999) 117
6. Aglietta M. et al., *Astrop. Phys.*, **10**, (1999) 1.; EAS-TOP Coll., Proc. 25th ICRC, Durban, **4**, (1997) 125; Navarra G. et al., *Nuclear Physics B (Proc. Suppl.)*, **60B**, (1998) 105.
7. M. Aglietta et al., Proc. 26th ICRC, Salt Lake City, **1**, 143
8. Capdevielle J.N. et al., *Kernforschungszen-trum Karlsruhe, KfK 4998*, (1992) (1999) 143